ELECTRONICS AND ELECTRICAL ENGINEERING
ISSN 1392 – 1215 *2011. No. 5(111)*
ELEKTRONIKA IR ELEKTROTECHNIKA

HIGH FREQUENCY TECHNOLOGY, MICROWAVES
T 191
AUKŠTŲJŲ DAŽNIŲ TECHNOLOGIJA, MIKROBANGOS

Electrodynamical Investigation of the Photonic Waveguide Structure

T. Gric
Semiconductor Physics Institute, Teraherzt's Electronics Laboratory,
A.Gostauto str. 11, LT-01108 Vilnius, Lithuania
L. Nickelson
Semiconductor Physics Institute, Teraherzt's Electronics Laboratory,
A.Gostauto str. 11, LT-01108 Vilnius, Lithuania,
Electronic System Department, Vilnius Gediminas Technical University,
Naugarduko str. 41, LT-03227 Vilnius, Lithuania, phone: +370 671 03291, e-mail: lucynickelson@gmail.com

Introduction

Photonic Crystal (PhC) based devices are being increasingly used in multifunctional, compact devices in integrated optical communication systems. They provide excellent controllability of light, yet maintaining the small size required for miniaturization. In [1] the silicon waveguide structures are investigated. Two structures that can be used in mid- and long-wave infrared regions: free standing and hollow core omnidirectional waveguides are investigated in [1].

The photonic crystals could be investigated by different methods. Thus the dielectric and metallic photonic crystals comprising the liquid crystal materials as defect layers or elements are investigated by the Finite Difference Time Domain method in [2].

There is a very limited amount of sources presenting the full electrodynamical analysis of the photonic and analogical structures [3–5].

Here we present the investigation of the photonic periodic waveguide structures using the Singular Integral Equations' Method. Our periodical waveguides consist of open (without metal screen) rectangular *n*-Si strip with rectangular holes inside it. We have investigated three kinds of waveguides which contain seven, five and three holes that are located throughout the entire length of the waveguide. It should be mentioned that we have used the complex permittivity of the material. The imaginary part of the permittivity depends upon frequency by this way

$$Im\,(\varepsilon_r^{Si})=1/(\rho\cdot 2\cdot\pi\cdot f), \qquad (1)$$

where ρ – is the specific electrical resistance, f – frequency.

The complex propagation constants have been calculated by the Muller's method in [6].

The Singular Integral Equations Method

Our investigated periodic waveguides cross-sections planes consist of the eight, six and four contours *L*. The expressions of all the electric field components which satisfy the boundary conditions by all the waveguide contours dividing the different waveguide materials are presented below. We apply the Krylov–Bogoliubov method whereby the contour *L* is divided into *n* segments and the integration along a contour *L* is replaced by a sum of integrals over the segments $j=1\ldots n$ [6]. The expressions of all electric field components for the area S^+ (the inner area of counter *L*) and S^- (the outer area of counter *L*) are presented below:

$$E_z^+ = \sum_{j=1}^{n} \mu_e^+(s_j) \int_{\Delta L} H_0^{(2)}(k_\perp^+ r')ds\,, \qquad (2)$$

$$E_z^- = \sum_{j=1}^{n} \mu_e^-(s_j) \int_{\Delta L} H_0^{(2)}(k_\perp^- r')ds\,, \qquad (3)$$

$$\left(E_x\right)^+ = -\frac{2\mu_0\mu_r^{Si}\,\omega cos\theta}{\left(k_\perp^+\right)^2}\mu_h^+(s_j) - i\mu_0\mu_r^{Si}\,\omega \Big/ \left(k_\perp^+\right)^2 \times$$
$$\times\left[k_\perp^+ \sum_{j=1}^{n}\left(\mu_h^+(s_j)\right)\int_{\Delta L} H_1^{(2)}(k_\perp^+ r')\frac{y_s-y_0}{r'}ds\right] +$$
$$+ ih\Big/\left(k_\perp^+\right)^2\left[k_\perp^+ \sum_{j=1}^{n}\left(\mu_e^+(s_j)\right)\int_{\Delta L} H_1^{(2)}(k_\perp^+ r')\frac{x_s-x_0}{r'}ds\right], \qquad (4)$$

$$\left(E_y\right)^+ = -\frac{2\mu_0\mu_r^{Si}\,\omega cos\theta}{\left(k_\perp^+\right)^2}\mu_h^+(s_j) - ih\Big/\left(k_\perp^+\right)^2 \times$$
$$\times\left[k_\perp^+ \sum_{j=1}^{n}\left(\mu_e^+(s_j)\right)\int_{\Delta L} H_1^{(2)}(k_\perp^+ r')\frac{y_s-y_0}{r'}ds\right] -$$
$$- i\mu_0\mu_r^{Si}\omega\Big/\left(k_\perp^+\right)^2\left[k_\perp^+ \sum_{j=1}^{n}\left(\mu_h^+(s_j)\right)^- \int_{\Delta L} H_1^{(2)}(k_\perp^+ r')\frac{x_s-x_0}{r'}ds\right], \qquad (5)$$

$$\left(E_x\right)^- = +\frac{2\mu_0\mu_{\mathrm{r}}^{\mathrm{a}}\,\omega\cos\theta}{\left(k_\perp^-\right)^2}\mu_h^-(s_j) - i\mu_0\mu_{\mathrm{r}}^{\mathrm{a}}\omega\Big/\left(k_\perp^-\right)^2 \times$$

$$\times\left[k_\perp^-\sum_{j=1}^{n}\left(\mu_h^-\left(s_j\right)\right)^-\int_{\Delta L}H_1^{(2)}(k_\perp^- r')\frac{y_s - y_0}{r'}ds\right] +$$

$$+ih\Big/\left(k_\perp^-\right)^2\left[k_\perp^-\sum_{j=1}^{n}\left(\mu_e^-(s_j)\right)\int_{\Delta L}H_1^{(2)}(k_\perp^- r')\frac{x_s - x_0}{r'}ds\right], \quad (6)$$

$$\left(E_y\right)^- = +\frac{2\mu_0\mu_{\mathrm{r}}^{\mathrm{a}}\,\omega\cos\theta}{\left(k_\perp^-\right)^2}\mu_h^-(s_j) - ih\Big/\left(k_\perp^-\right)^2 \times$$

$$\times\left[k_\perp^-\sum_{j=1}^{n}\left(\mu_e^-(s_j)\right)\int_{\Delta L}H_1^{(2)}(k_\perp^- r')\frac{y_s - y_0}{r'}ds\right] -$$

$$-i\mu_0\mu_{\mathrm{r}}^{\mathrm{a}}\,\omega\Big/\left(k_\perp^-\right)^2\left[k_\perp^-\sum_{j=1}^{n}\left(\mu_h^-(s_j)\right)\int_{\Delta L}H_1^{(2)}(k_\perp^- r')\frac{x_s - x_0}{r'}ds\right], \quad (7)$$

here $\mu_e(s_j)$ and $\mu_h(s_j)$ are functions at the same contour point are different for the field components in the areas S^+ and S^-, i.e. $\mu_h^+(s_j) \neq \mu_h^-(s_j)$. The magnitude $H_0^{(2)}$ is the Hankel function of the zeroth order and of the second kind, $H_1^{(2)}$ is the Hankel function of the first order and of the second kind. Here complex magnitudes $k_\perp^+ = \sqrt{k^2\varepsilon_{\mathrm{r}}^{\mathrm{Si}}\mu_{\mathrm{r}}^{\mathrm{Si}} - h^2}$ and $k_\perp^- = \sqrt{h^2 - k^2\varepsilon_{\mathrm{r}}^{\mathrm{a}}\mu_{\mathrm{r}}^{\mathrm{a}}}$ are the transversal propagation constants of the *n*-Si medium in the area S^+ and in the air area S^-, correspondingly. Here $h = h' - ih''$ is the complex propagation constant where h' is the phase constant and h'' is the attenuation constant (waveguide losses). The magnitude k is the wave number in a vacuum. The segment of the contour L is $\Delta L = L/n$, where the limits of integration in the formulae (2–7) are the ends of the segment ΔL. The angle θ is equal to $g\cdot 90°$ with g from 1 till 4, if the contour of the waveguide cross-section is a rectangular one, as a result can be $\cos\theta = \pm 1$ and $\sin\theta = \pm 1$ in the formulae (4–7).

We can obtain the transversal components of the magnetic field H_x and H_y using SIE method in the form analogical formulae (2–7).

After we know all EM wave component representations in the integral form we substitute the component representations to the boundary conditions. We obtain the homogeneous algebraic equations' system with the unknowns $\mu_e^+(s_j)$, $\mu_h^+(s_j)$, $\mu_e^-(s_j)$ and $\mu_h^-(s_j)$.

The condition of solvability is obtained by equalizing the determinant of the complex system to zero. The roots of the system let us to determine the complex propagation constants of the main and higher modes of the waveguide. For finding the complex roots of the complex determinant we have used the Müller's method. Müller's method uses 3 initial guesses x_0, x_1, x_2 and determines the intersection with the x axis of a parabola. Note that this is done by finding the root of an explicit quadratic equation. After obtaining the propagation constant of some required mode the determination of the electric and magnetic fields of the mode becomes possible. For the correct formulated problem [7] the solution is one–valued and stable with respect to small changes of the coefficients and the contour form [8].

The approbation of the computer softwares

We have created the computer software based on the method SIE in the MATLAB language. This software let us calculate the dispersion characteristics of waveguides with very complicated shapes of cross-sections. The computer software was approbated by comparison with data of different published sources, for example, the dispersion characteristics of the rectangular dielectric waveguide [9] and the dielectric waveguide with the metal strip line [8]. In Fig. 1 the dispersion characteristics of the open rectangular dielectric waveguide with sizes of its sides $(15\text{x}5)\cdot 10^{-3}$ m and the waveguide material permittivity equal to 2.06 are presented. We see the main mode and three higher modes that can propagate in the dielectric waveguide. Our calculations are the solid lines and the results from [9] are presented with points.

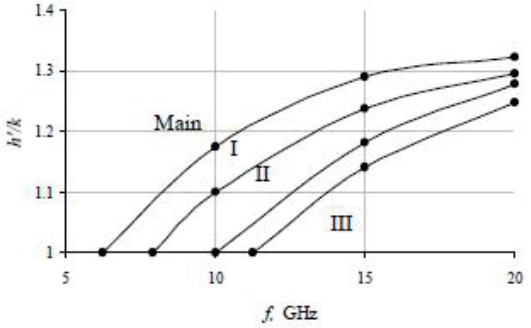

Fig. 1. Comparison of the dispersion characteristics of the rectangular dielectric waveguide calculated by presented here SIE algorithm and data from [9]

In Fig. 2 the sizes of the dielectric waveguide with the metal strip line are the following: $d = 3.17\cdot 10^{-3}$ m, $w = 3.043\cdot 10^{-3}$ m, $l_1 = l_2 = 5\cdot 10^{-3}$ m, $t = 3\cdot 10^{-6}$ m. The permittivity of the microstrip line substrata is 11.8. Our calculations are shown with dots (the main mode), with triangles (the first higher mode) and with circles (the second higher mode). In Fig. 2 the data from the book [8] is shown by the solid line (the main mode), dashed line (the first higher mode), dash-dotted line (the second higher mode).

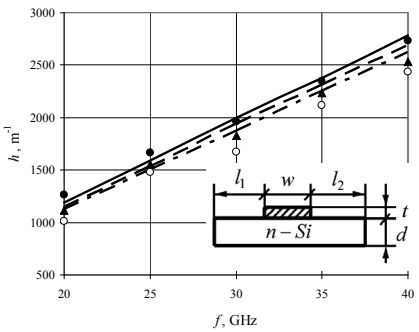

Fig. 2. Comparison of the dielectric waveguide with the metal strip line dispersion characteristics calculated by presented here SIE algorithm and data from [8]

The difference between our results and data from the book [8], page 195 can be explained by the following way. The presented articles calculations were fulfilled in the MATLAB language with a high-level precision in the contrast to the lower accuracy FORTRAN77 that was used in [6].

In Fig. 1 and Fig. 2 we can see that an agreement of the compared results is good. This confirms the correctness of algorithm proposed in this work.

The investigation of the periodic *n*-Si waveguide structure

Here we present the investigations of the 2D periodic *n*-Si waveguide structure with the plot of the cross section equal to 5x5 mm^2 (see Fig. 3). All the sizes, indicated in the figure can be chosen arbitrary and are the independent variables from each other.

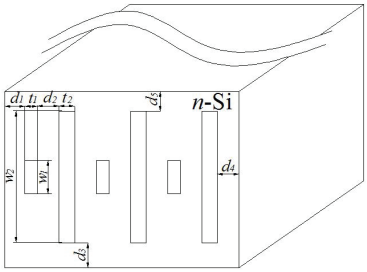

Fig. 3. The periodic *n*-Si waveguide structure

We selected several sizes that remain constant in our calculations. They are the following $t_1 = t_2 = 0.2$ mm, $w_1 = w_2 = 1$mm, $d_2 = 0.2$ mm. Here the sizes of all holes are $w_n \times t_n = 1 \times 0.2\ mm^2$, where n can be till seven in our calculations. The real part of the complex permittivity of the base waveguide semiconductor material *n*-Si is equal to 11.8. The imaginary part of the complex permittivity is calculated using the formulae (1). The specific resistance ρ is 100 Ω·m.

The dispersion characteristics of the investigated waveguide structure are presented in Fig. 4 and 5. The dispersion characteristics were calculated when the number of the holes is different (7, 5, 3 holes). All the holes are located in the center of the waveguide. Therefore $d_1 = d_4$ in all the cases. The case when the waveguide has a number of holes equal to 7 is displayed by the dashed line and d_1=1.2 mm. The case with the number of holes equal to 5 is displayed with dots and d_1=1.6 mm. The last case with the number of holes equal 3 is shown by the solid line. In this case d_1=2 mm.

In Fig. 4 the dispersion characteristics of *n*-Si waveguide when the holes are located symmetrically correspondingly to the top and bottom of waveguide cross-section are shown. In this case the dimensions are equal to $d_3 = d_5 = 2$ mm.

In Fig. 4 we see that there are peaks of maximum at some frequencies (f = 40 GHz) for waveguides with three, five and seven holes. The largest losses are observed for the waveguide with 5 holes at f = 40 GHz.

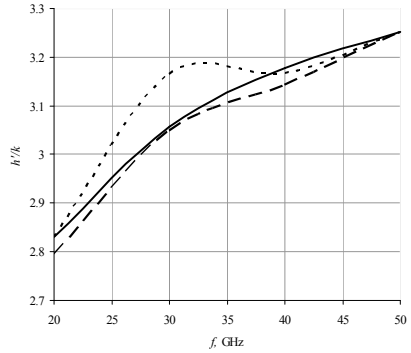

a)

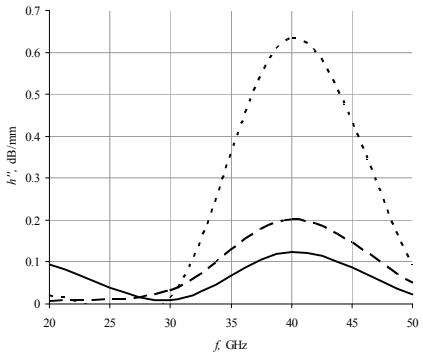

b)

Fig. 4. The dispersion characteristics of the periodic waveguide structure with $d_3 = d_5 = 2$ mm: a – the dependence of the phase constant; b – the dependence of losses upon frequency

We see that the smallest losses are observed for the waveguide with 5 and 7 holes in the frequency range 20–30 GHz.

Thus we can add the air holes in the waveguide cross-section in order to reach the suitable characteristics for creating of some devices as filters, absorbers, modulators etc. In other words we can carry out the optimization of waveguide characteristics.

In Fig. 5 we present the dispersion characteristics of the photonic crystal with air holes shifted in the vertical direction. At this case the vertical distances of holes from the top and bottom of the *n*-Si substrate are equal to d_3=3.5 mm, d_5 = 0.5 mm.

Comparing Fig. 4 and fig. 5 we see that the normalized propagation constants h'/k of the both structures are approximately at the same range from 2.8 till 3.3.

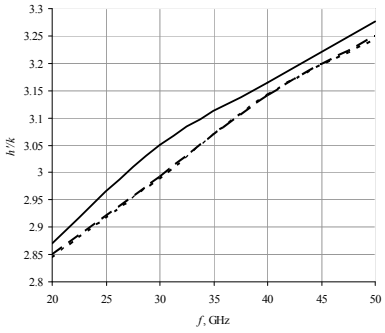

a)

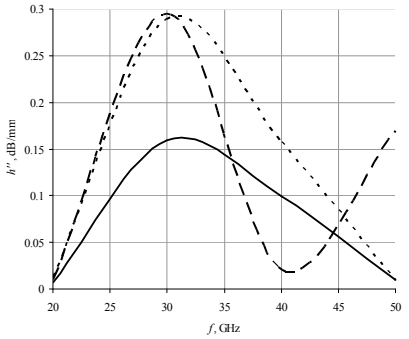

b)

Fig. 5. The dispersion characteristics of the periodic waveguide structure with the moves air holes when d_3=3.5 mm, d_5 = 0.5 mm: a – the dependence of the phase constant; b – the dependence of losses upon frequency

Conclusions

1. We have carried out the rigorous electrodynamical analysis of dispersion characteristics of the photonic waveguide with holes inside of semiconductor *n*-Si substrate.
2. We investigated dependencies of losses on the quantity of holes and their location with respect to the top and the bottom sides of the semiconductor substrate.
3. We have discovered that the loss maximum shifts from frequency f=40 GHz till f=30 GHz when the distance d_5 change from 2 mm till 0.5 mm.
4. The comparison of waveguide dispersion characteristics with symmetric (d_3=d_5=2 mm) and asymmetric (d_3=3.5 mm, d_5=0.5 mm) location of holes inside of semiconductor substrate shows that especially considerably changes the losses' behavior.

References

1. **Stankovic S., Milosevic M., Timotijevic B., Yang P.Y., Teo E.J., Crnjanski J., Matavulj P., Mashanovich G.Z.** Silicon photonic waveguides for near– and mid–Infrared regions // Acta Physica Polonica A, 2007. – Vol. 112(5). – P. 1019–1024.
2. **Kosmidou E. P., Kriezis E. E. and Tsiboukis T. D.** FDTD analysis of photonic crystal defect layers filled with liquid crystals // Optical and Quantum Electronics, 2005. – Vol. 37. – P. 149–160.
3. **Djavid M., Ghaffari A., Monifi F., Abrishamian M. S.** Photonic crystal narrow band filters using biperiodic structures // Journal of Applied Sciences, 2008. – Vol. 8(10). – P. 1891–1897.
4. **Eidukas D., Kalnius R.** Multiparameter Electronic Tools Quality Level Linear Transformation Models // Electronics and Electrical Engineering, 2010. – Vol. 105(9). – P. 23–27.
5. **Asmontas S., Nickelson L., Bubnelis A., Martavicius R., Skudutis J.** Hybrid Mode Dispersion Characteristic Dependencies of Cylindrical Dipolar Glass Waveguides on Temperatures // Electronics and Electrical Engineering. – Kaunas: Technologija, 2010. – Vol. 10(106). – P . 83–86.
6. **Gric T., Nickelson L., Asmontas S.** Electrodynamical characteristic particularity of open metamaterial square and circular waveguides // Progress In Electromagnetics Research, 2010. – Vol. 109. – P. 361–379.
7. **Gakhov F. D.** The boundary problems, Science, Moscow – 1977.
8. **Nickelson L., Shugurov V.** Singular integral equations' method for the analysis of microwave structures. – VSP Brill Academic Publishers, Leiden–Boston, the Netherlands, 2005.
9. **Ikeuchi M., Sawami M., Niki H.** Analysis of open–type dielectric waveguides by the finite–element iterative method // IEEE Trans., 1981. – Vol. MTT–29(3). – P. 234–239.

Received 2011 02 15

T. Gric, L. Nickelson. Electrodynamical Investigation of the Photonic Waveguide Structure// Electronics and Electrical Engineering. – Kaunas: Technologija, 2011. – No. 5(111). – P. 3–6.

Presented the electro dynamical analysis of the *n*-Si photonic waveguide structures. The rigorous solution of the problem was fulfilled by the Singular Integral Equations' method (SIE) using the Muller's method. Here the dispersion characteristics of six different structures with three, five and seven air holes are analyzed. The air holes are located symmetrically to the centre of the waveguide substrate in the first three structures. The air holes are shifted in the other examined structures. In the article dependencies of the phase constants and losses on the number of holes and their location with respect to the top and the bottom sides of the semiconductor substrate are presented. The dispersion characteristics' comparison of waveguides with the different location of holes inside *n*-Si substrate shows that especially strong dependences are observed in the behaviour of losses. Ill. 5, bibl. 9 (in English; abstracts in English and Lithuanian).

T. Gric, L. Nickelson. Fotoninės bangolaidinės struktūros elektrodinaminė analizė // Elektronika ir elektrotechnika. – Kaunas: Technologija, 2011. – Nr. 5(111). – P. 3–6.

Pateikiama n-Si fotoninių bangolaidinių darinių elektrodinaminė analizė. Elektrodinamikos uždavinio griežtas sprendinys gautas taikant singuliariųjų integralinių lygčių ir Mullerio metodus. Ištirtos šešių įvairių darinių su trimis, penkiomis ir septyniomis skylėmis, užpildytomis oru, dispersinės charakteristikos. Pirmuoju atveju skylės yra išdėstytos simetriškai bangolaidžio centrui. Antruoju atveju skylės yra pastumtos bangolaidžio centro atžvilgiu. Apskaičiuotos fazinių pastoviųjų ir nuostolių priklausomybės nuo dažnio esant įvairiems skylių matmenims ir padėčiai. Lyginant bangolaidinių darinių su skirtingai išdėstytomis skylėmis dispersines charakteristikas nustatyta, kad nuostolių priklausomybei nuo dažnio ypač didelę įtaką turi skylių dydžiai ir padėtis. Il. 5, bibl. 9 (anglų kalba; santraukos anglų ir lietuvių k.).